

Fig. S1. Spatial correlation coefficients between GPP and temperature (T2M) for three observational datasets (GLASS, GOSIF, JUNG) and 17 TRENDY models. For each grid, correlation coefficient is calculated between annual GPP and meteorological factors through 1982-2017 for GLASS, 2001-2018 for GOSIF, or 1982-2011 for JUNG.

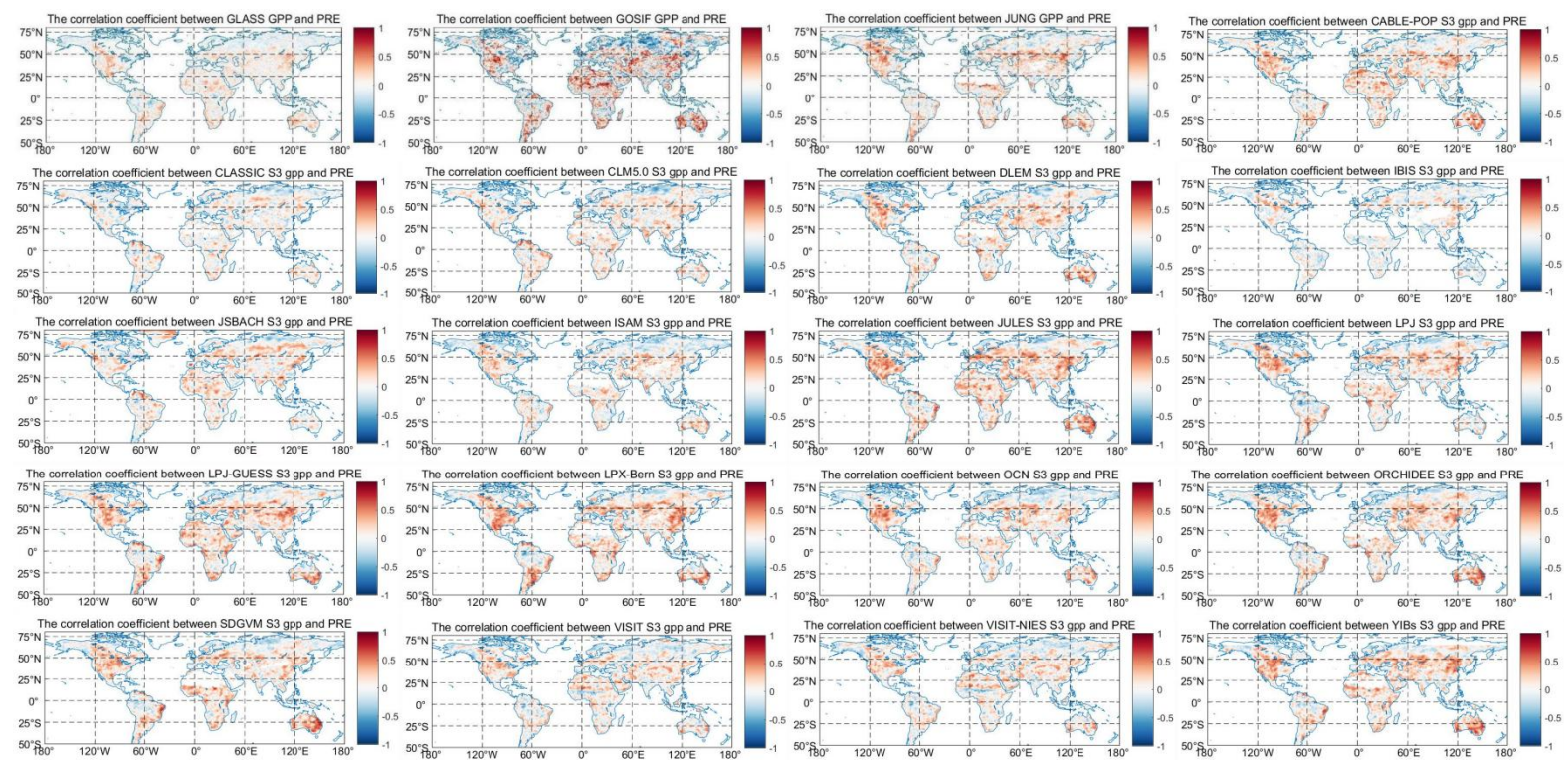


Fig. S2. The same as Fig. S1 but for correlations between GPP and precipitation (PRE).

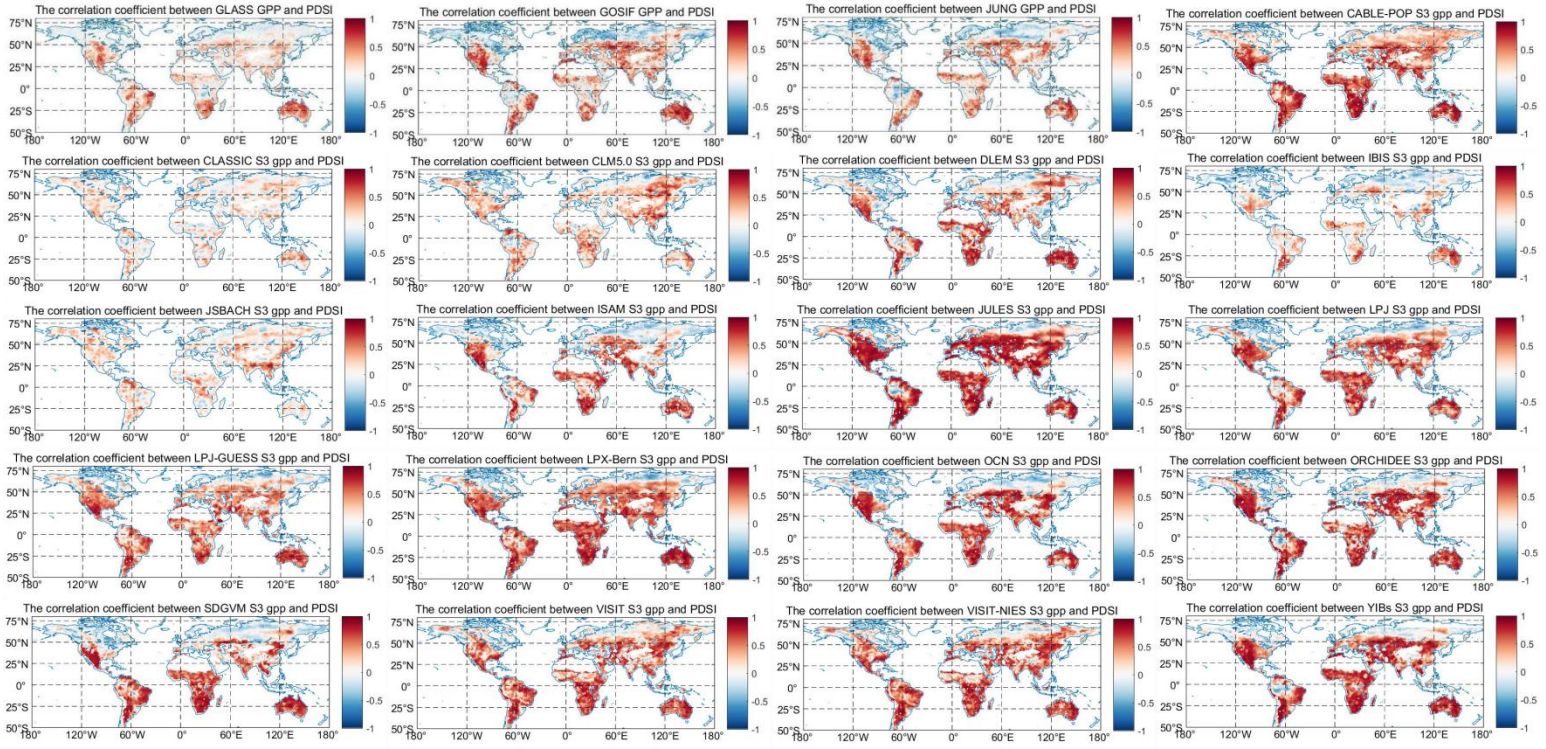


Fig. S3. The same as Fig. S1 but for correlations between GPP and self-calibrated Palmer Drought Severity Index (scPDSI).

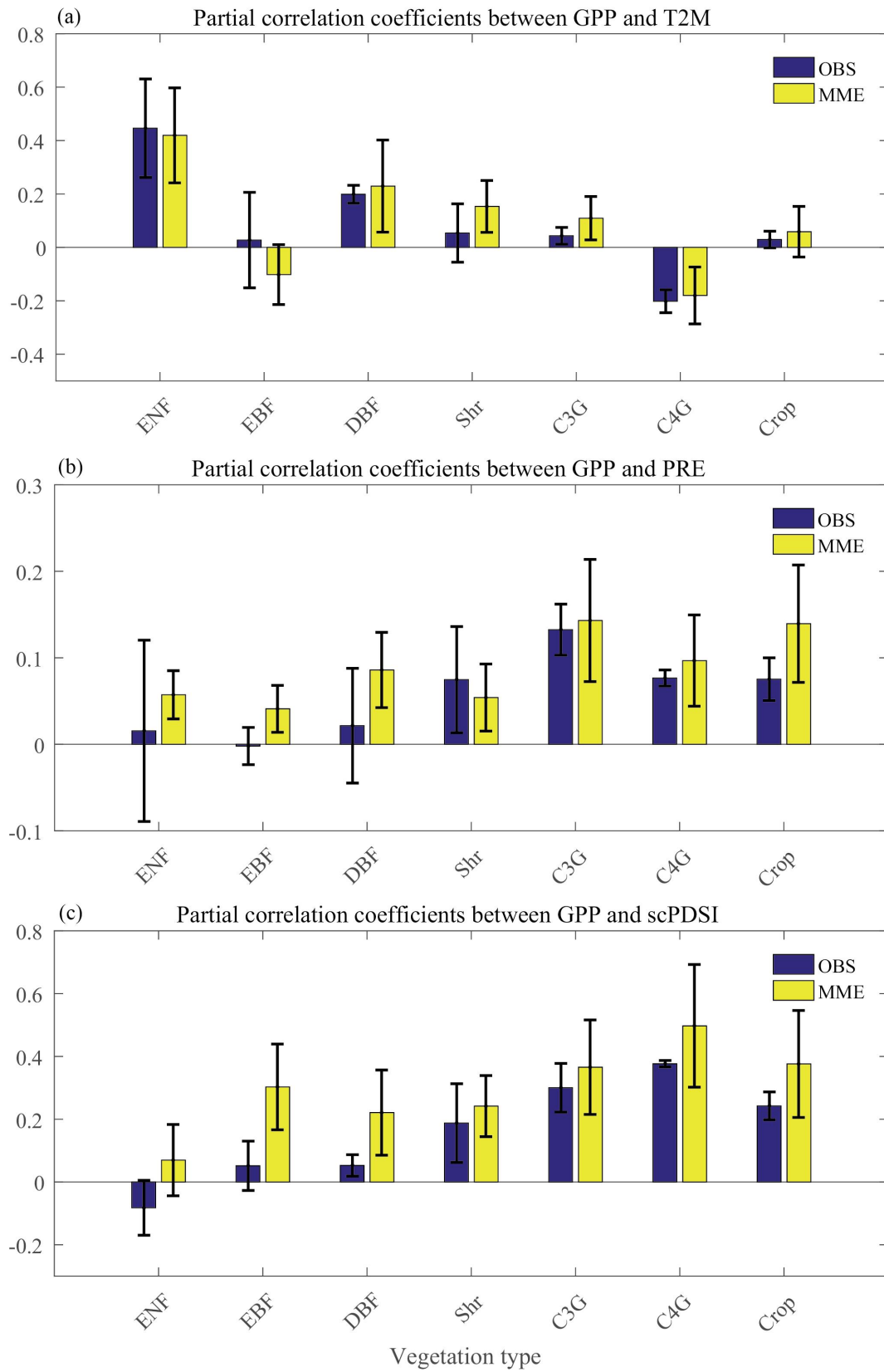


Fig. S4. Partial correlation coefficients between GPP and meteorology averaged for different vegetation types. The correlations are calculated between GPP and (a) T2M, (b) PRE, and (c) scPDSI for both observations (blue) and models (yellow). The mean of three observational products and multiple models are presented with the errorbar indicating one standard deviation for either observations or models.

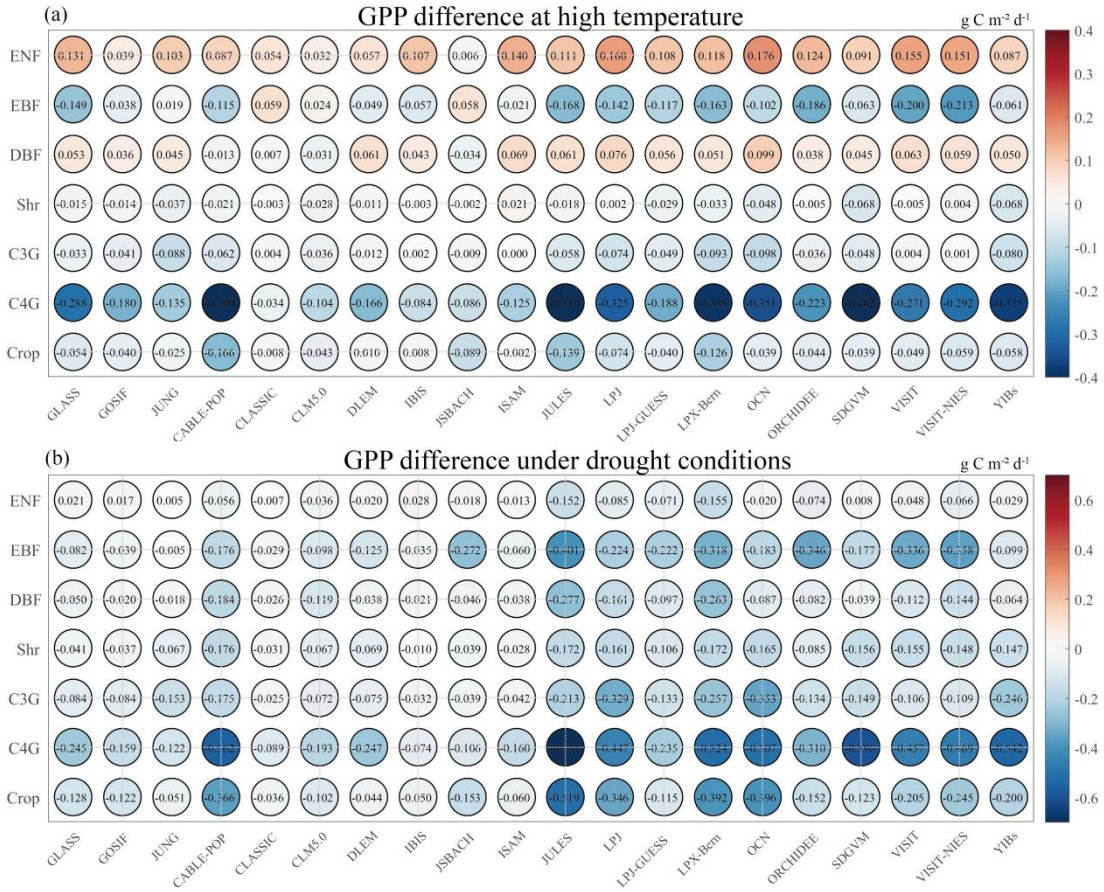


Fig. S5. Heatmaps of GPP responses to extreme (a) warming and (b) drought across different vegetation types. Changes in GPP are shown for years with the top 10% of (a) highest temperatures and (b) lowest scPDSI values, relative to the mean state, based on three observational datasets (GLASS, GOSIF, and JUNG) and 17 vegetation models. Vegetation types include evergreen needleleaf forest (ENF), deciduous broadleaf forest (DBF), evergreen broadleaf forest (EBF), shrubland (Shr), C_3 grassland (C3G), C_4 grassland (C4G), and cropland (Crop).

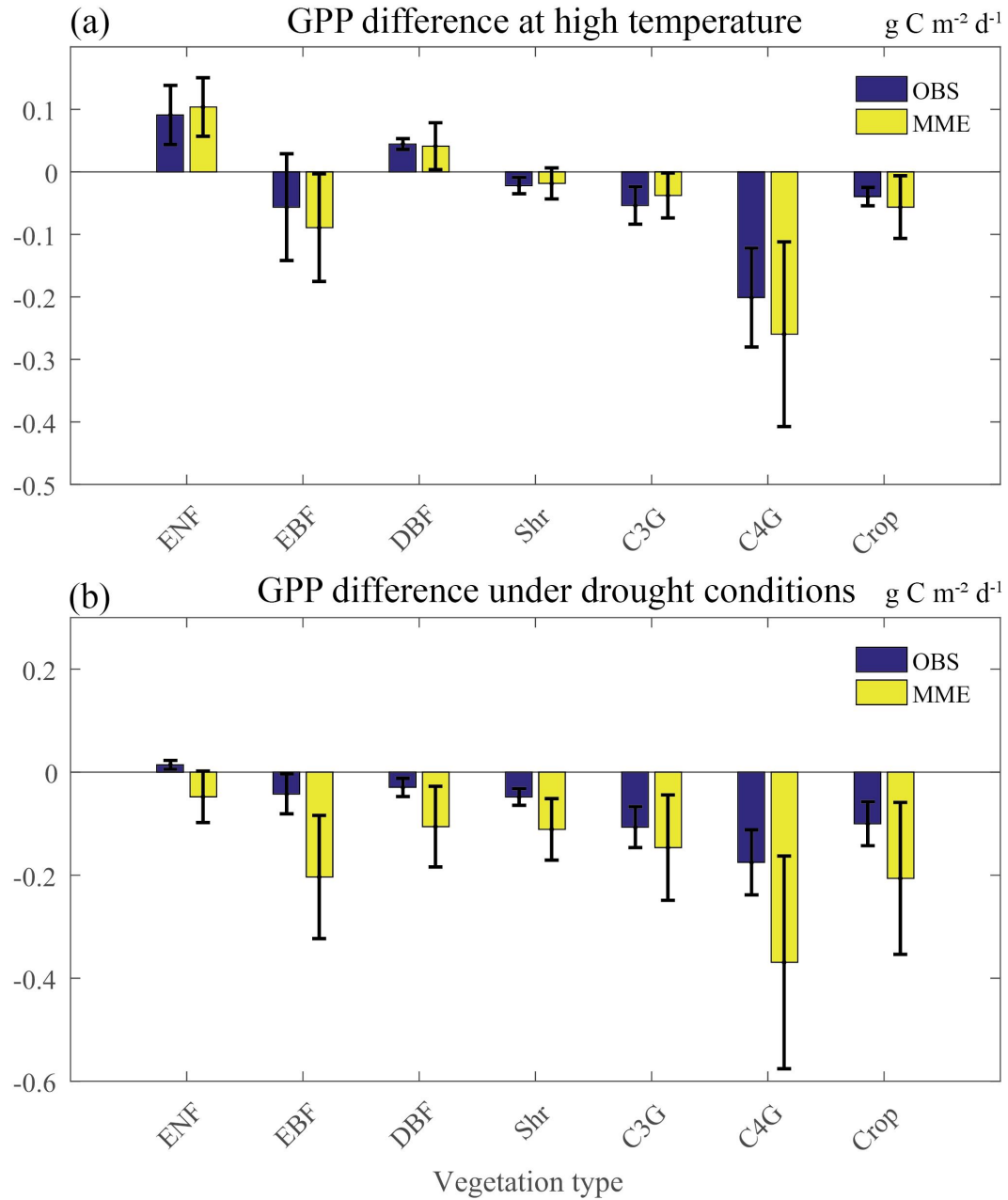


Fig. S6. GPP responses to extreme warming and drought conditions across vegetation types. Differences in GPP are calculated as deviations during years with the top 10% (a) highest temperature or (b) lowest scPDSI values, relative to the long-term mean, for individual grids. These differences are aggregated by seven vegetation types and averaged for three observational datasets (blue) and the multi-model ensemble mean (yellow). The Error bars indicate one standard deviation across observational datasets or models.

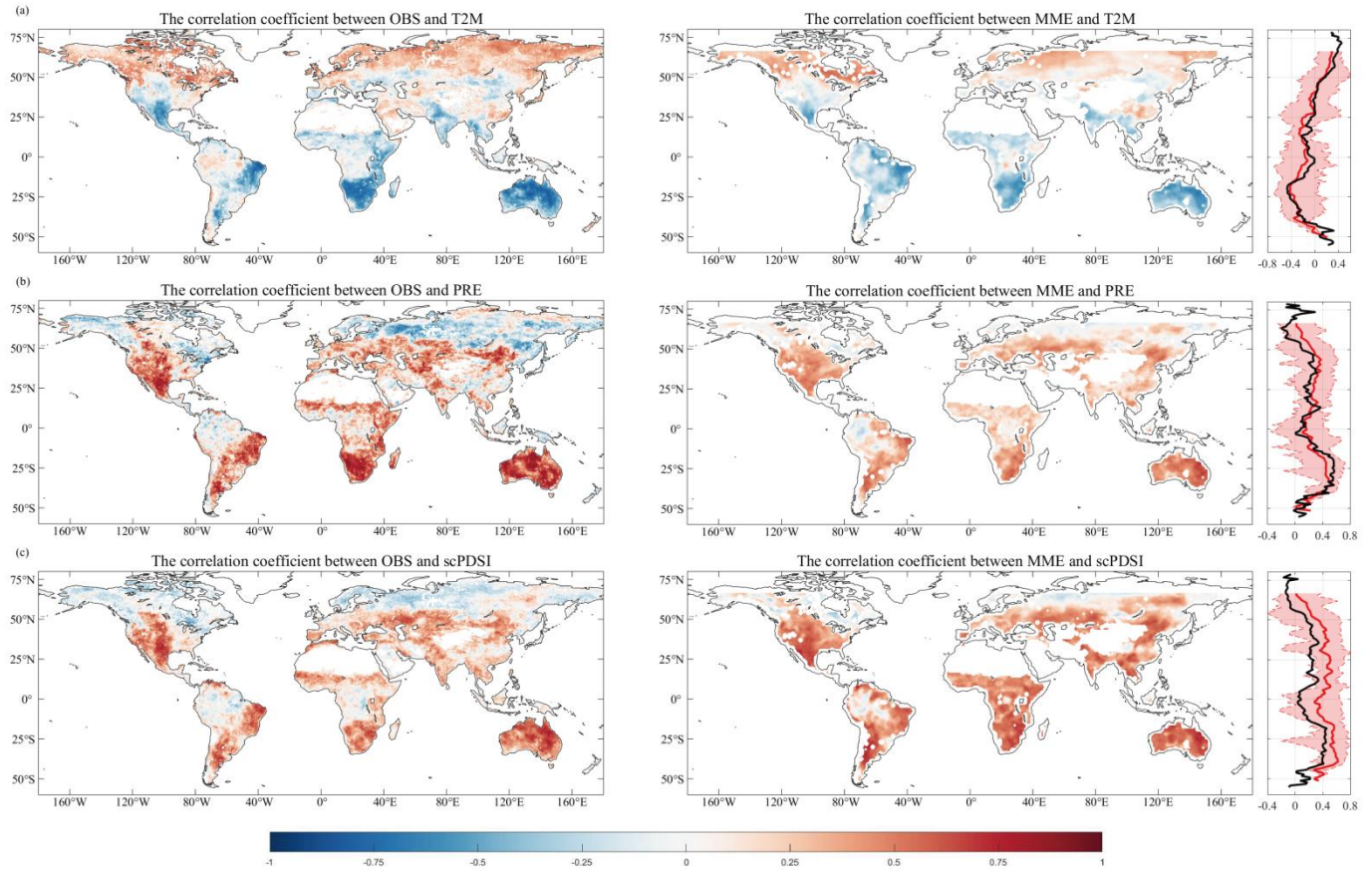


Fig. S7. Mean spatial correlation coefficients between GPP and (a) T2M, (b) precipitation (PRE), and (c) scPDSI averaged for three observational datasets (GLASS, GOSIF, JUNG) and multiple models. For each grid, correlation coefficient is calculated between annual GPP from S2 simulations and meteorological factors through 1982-2017 for GLASS, 2001-2018 for GOSIF, or 1982-2011 for JUNG. Latitudinal variations in correlation coefficients are also shown, with observational data in black and model simulations in red; shading indicates one standard deviation.

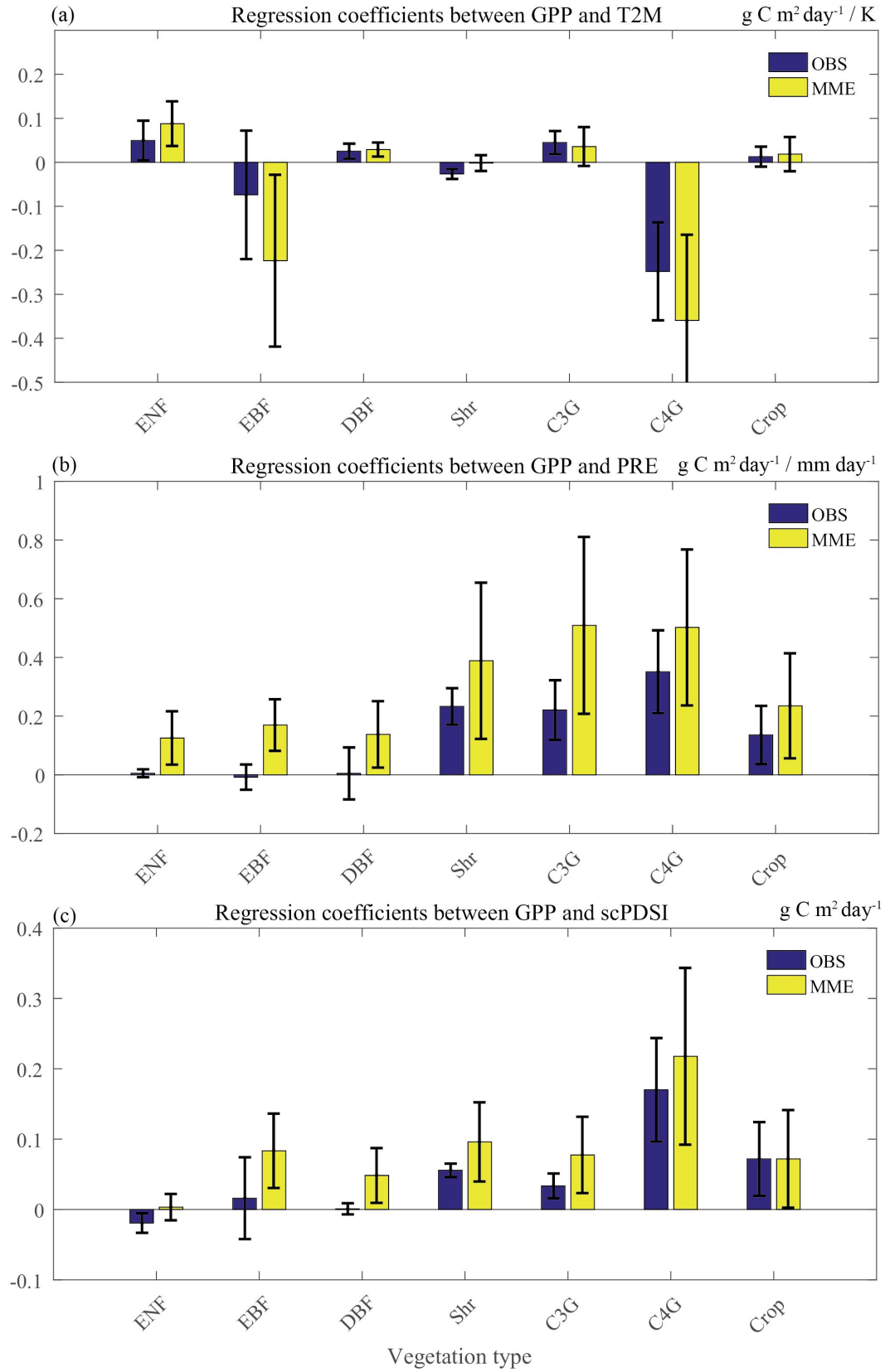


Fig. S8. Linear regression coefficients between GPP and meteorology across different vegetation types. The regression coefficients are calculated between GPP and (a) T2M, (b) PRE, and (c) scPDSI for both observations (blue) and models (yellow). The mean of three observational products and S2 simulations by multiple models are presented with the errorbar indicating one standard deviation for either observations or models.